# The asynchronous growth and movement reconstruction of the early molting animals

**Tian Lan** ( lantianing@sina.com )
Guizhou University https://orcid.org/0000-0001-7713-5411
**Daniel Meulemans Medeiros**
University of Colorado

**Research article**

**Keywords:** Epithelium, Cell mechanics, asynchronous growth, movement, Ecdysozoa

**Posted Date:** September 10th, 2020

**DOI:** https://doi.org/10.21203/rs.3.rs-44294/v2

# Abstract

Epithelium is one of the basic types of animal tissue, and forms tissue boundaries that act as physical barriers to separate adjacent cell clusters. However, tissue boundaries at cellular resolutions can hardly be found in the fossil record. Here we focus on the growth and movement patterns of early Ecdysozoans by quantifying cell-level forces in the epithelium of two worms from the early Cambrian and Ordovician period. The arrangement of the epithelium cells (that do not necessarily represent biological cells) separating the body rings of these early Ecdysozoans indicates precise morphological patterning at the cellular level was established in the early Cambrian. The force distribution patterns on the body ring further suggest that the boundary cells helped maintain a pressure gradient between the rings, consistent with a role in movement. Finally, the active tension field of the worms plates throughout their ontogeny, and steady state of their epithelium cells, indicate these molting animals employed an asynchronous growth pattern in their epithelium.


# 1. Introduction

Growth and movement are two basic proprieties of animals. The growth patterns of a living organism can be reconstructed by analyzing the mechanical forces underlying its development [1]. Peristaltic movement is widely employed by the worms living near sediment/water (air). Worms using peristaltic movement have an epithelial system that displays a tension – compression rhythm [2] with relatively high potential energy. In contrast, when in a steady state and not involved in movement, epithelial cell clusters minimize their potential energy [3].

In a physical perspective, the forms of living beings are created by cell movements. Recent studies quantifying forces in cell proliferation, sorting and other developmental processes, showed that physical forces also contribute to maintain boundaries [4-6]. The mechanical properties of cell lattices have been quantitatively described [7]. Most of the cell boundaries are relatively straight. Comparatively, the leaf epidermal cells with puzzles and pavements of the cell boundary increase the contact area of the neighboring cells and strengthen the structural integrity of the epithelium. The pavement cell form corresponds to higher grade anatomical structures and recently pavement cells have been found in the 535 ma worms fossil cuticles [8].

In a larger scale, segments can be regarded as periodically organized cell clusters. The segment number varies considerably among species, ranging from six in some frogs to several hundred in snakes. It is known that physical cues, like mechanical stretching, can induce the formation of additional somites in the vertebrate embryo [9]. Similarly, some larval worms will add from 80 to more than 300 rings during development [10]. The maintenance of straight and sharp boundaries of the segment is crucial for subsequent patterning events.

Segmentation step wisely evolves in organ systems. Epithelium derives from ectoderm and it can segment normally without the mesoderm [11], suggesting epithelium segmentation is regulated

independently from mesodermal segmentation [12]. Segmentation may have evolved to improve locomotion in arthropods, annelids and chordates [13]. The Cycloneuralians display epithelial segmentation and remarkable biodiversity in the Cambrian–Ordovician period [14-16].

# 2. Material And Methods

In this study, the definition of the cell includes, but is not restricted to, the biological cell. Two new species of the stem group Cycloneuralia of the early Paleozoic period were reported. Both fossils' surface displays fine polygonal structures on the scale of biological cells. Here we use the light microscope Leica 205C and scanning electron microscope to photograph the specimens.

The vertex model was employed to describe cell clusters states within the epithelium of the worms. In the vertex model, the epithelial shape is represented by a set of vertices that mark the common point of three or more neighboring cells. It was initially used to study the packing of bubbles in foams, then adapted to study the 2D packing and rearrangement of apical cell surfaces in the planar epithelium [17].

- **Image segmentation**

We use the watershed algorithm [18] of Image J to segment the cells. Initial scanning electron microscope (SEM) images of the worm fossils were smoothened to reduce the noise and facilitate the cell boundary segmentation.

- **Cell mechanical analysis**

The processed images were load in the CellFIT to reconstruct the force field of the cell cluster [19]. Cell boundaries were generated from uniformly spaced mesh points at each edge in order to obtain ideal triplet approach angles for calculating forces.  A cell is not represented by a polygon, but by a polyarc.

The key equation of CellFIT is for any particular triplet junction to be in equilibrium, the adjacent cell edges satisfy the force balance equation:

$\Sigma \gamma_{mn} r_{mnA} = 0$

where the unit vectors $r_{mnA}$ are constructed tangent to the limiting angle at which the membrane along the boundary between cells m and n approaches the triple junction and pointing away from the junction, and the summation is carried out over all edges that connect to the triple junction. The $\gamma_{mn}$ values are the corresponding unknown membrane tensions [19].

The Laplace's equation is used to solve the pressures fields of the system,

$\Delta p = \gamma (1/R_1+1/R_2)$

Δp is the pressure difference between cells. *γ is the parameter of the surface tension.* R is the radius of curvature of the cells. Base on these equations [19], the tension and pressures fields of the study area of the cell clusters were solved by CellFIT .

# 3. Systematic Palaeontology

**Cycloneuralia**

**Stem group**

***Jinia rosettea* gen. et sp. nov.**

**Etymology.** The generic name derives from the the Jindinshan formation, the strata where the fossil been found. Species name is after the rosette shape formed by the plate and its surrounding polygons (Figure 1*a-d*; S1).

**Holotype.** Guizhou Research Center for Palaeobiology (GRCP) 14001, Guizhou University . GRCP 14002, 14003 includes worm at different developmental stages.

**Locality and horizon.** The specimens were collected from the lower mudstone of the Jindinshan Formation, Cambrian Stage 4, of Guizhou, South China.

**Diagnosis for genus and species.** The body of the worm are made up of rings. Each ring boundary is defined by annular furrows (Figure 1*b,c*; 4*a,b*; S1). Linearly arranged circular plates with apexes are distributed on the two sides of the furrow (Figure 1*b*; S1*g*). The furrows consist of bi-serial oval formed polygons, named boundary cells. The surface of the epidermis dominated by 4 – 8 sided cell lattices (Figure 1*d*; S1*g*). The boundary of the plates and cell lattices are zigzag shaped (Figure 1*c*, *d*; S1*d*).

**Remarks**: Convergent evolution likely forces several clades to fall into a close morpho space. The inter plate polygons have been found in the phosphatized epithelial fragments of *Hadimopanella* in which named the micro plates and the boundary cells were previously named “inter annular furrows” [20, 21]. These structures have received less attention than the plate. The small specimens have a relatively narrow inter plate space, while the space extends in the larger specimens (Figure S1). The specimen series is interpreted as a developmental sequence of the *J. rosettea.* New inter plate cell lattices emerge (Figure S1). The developmental patterns are widely recorded in other early Cycloneuralia [22].

***Meitis elegans* gen. et sp. nov.**

**Etymology.** The generic name derives from the the Meitan formation, the strata that the fossil been found. Species name after elegance.

**Holotype.** Guizhou Research Center for Palaeobiology (GRCP) 22001, Guizhou University (Figure 1*e*).

**Locality and horizon.** The specimen was collected from the lower mudstone of the Meitan Formation, Early Ordovician (Florian), Guiyang city, South China.

**Dignosis for genus and species.** The body of the worm is made up of rings. Each ring boundary is defined by annular furrows (Figure 1*f,g*; 4*c,d*). The annular furrows consist of rectanglar polygons. The platelets are distributed along the two sides of a row of rectangle polygons. The surface of the epidermis dominated by 6 sided cell lattices (Figure 1*f*). The aspect ratio of the plate range is from 1 - 2 ,and the apexes of the plates range from 1 to 3 (Figure 1*g*).

**Remarks**: The ornaments of the epidermis of the Ordovician worms [23] occupied a much wider morphospace than that of their Cambrian counterparts. *Meitis elegans* gen. et sp. nov. share similarities with the plate outline of the 495-Myr-old *Palaeoscolex piscafumm* and *Gnmoscolex* herodes from the lower Ordovician strata. All of them have distinct boundary zone of the rings [24, 25]. However, the plate apexes and distribution pattern of these species are remarkably different [24, 25].

# 4. Results

### (a) Comparative anatomy

Four cuticular elements: plates, platelets, amorphous polygons and linearly arranged polygons are found on the fossil epithelium (Figure 1,2). The shape and size of the cell lattices of the worms are reminiscent of the epithelial cells of extant animals (Figure 2*a*) and their polygonal relics could be observed on the inner surface of the cuticles (Figure S1*b,c*). We thus treated each polygon as likely representing single cells rather than subcellular structures, or muticellular ornaments. The linear formed polygons are interpreted as the boundary cells (BCs) that separate each ring. The BCs of *J. rosettea* are biserial and oval shaped. Comparatively, BCs of the *M. elegans* are uniserial and rectangle shaped (Figure 1*b,g*). The *J. rosettea* epithelium is dominated by 4 – 8 sided cell lattices (Figure 1*c,d*) with zig zag shaped boundaries. The cell lattices of *M. elegans* are mainly hexagons, and the cell boundaries are relatively straight (Figure 1*g*).

### (b) Growth and movement pattern reconstruction

The study used a quantitative approach to understand the growth pattern of the epidermal cell grade structures of the worms by analysizing the force fluctuation landscapes of the cell clusters [26]. Growth

and movement processes potentially affect the tension and pressure field of the cells. The tension field was treated as the proxy for the growth rate within a ring [26, 27] (Figure 2). The platelets and plates were regarded as a developmental continuum in the case of the early worms (Figure 1*g*; Figure 2*b-d*). The developing plate was interpreted as a hot spot of the tension field (Figure 2*b-d*). Conversely, the cell polygons reflect the relaxed network configuration (Figure 2*e,f*), and represent the steady state of the epithelial system of the early molting animals [3].

The tension is unequally distributed around the worms' plates (Figure 2*b–d*) similar to the mitosis loop [28] of the epidermal cells, with the new cells proliferating from the hot spot where a relatively high tension value is recorded (Figure 2*a*) [28]. While the plate is not a mitosis loop, and does not necessary represent a single cell, , the nonequilibrium tension fields of the plates suggest they are in an active state. More broadly, the asymmetric distributions of the tension field are found within the mesh like plates of the *Microdictyon* (Figure 3) [29]. Under the assumption that tension correlates positively to the growth rate, the results suggest allometric growth of the early worm's epithelial elements.

The pressures are unequally distributed on the two sides of the BCs (Figure 4*b, d*), suggesting the boundary cell prevents pressure transmission to the region's base on the 2D lattices analysis (Figure 4*e*). The cells density of BCs region is higher than that of the surrounding cells which resistance to nonequivalent stress field and the tissue under pressure tends towards a uniform cell organization (BCs) [30].

# 5. Discussion

- **asynchronous growth pattern**

Some clades (tardigrata, onychophora etc.) employed an incomplete molting pattern. Hard epidermal derivatives (jaws, claws, dorsal spines etc.) have a cone-in-cone construction [31]. The desynchronization of molting ensures stiffness of these functional elements (feeding, climbing and protection etc.) throughout the lifetime of the organisms. This system tends to relax to the minimum energy state in the plate-free region of the ring (Figure 2*e,f*). The developing plates formed like volcanic islands interspersed among the inactive epithelial ocean. Thus, we suggest the early worms employed an asynchronous growth pattern in their epithelium. Simulation experiments reveals the cell types with lower tension will envelop the cell clusters with higher cortical tension [32].

The epithelial sheet are three dimensional (3D) in reality, and 3D-preserved specimens [14] (Figure 4*g*; S1 *b,c,f*) show the boundary region of the worms is slightly curved. The annuli/furrow patterns are widely observed in worm-like animals. Previous work shows differential tension drives epithelial cell ingression [33]. Our results show the consequence of the ingression: The boundary cells prevent pressure transmission to the adjustment region,  establishing pressure gradients beween the rings (Figure 4), which is the basis of peristaltic movement. The pressure field was used as a proxy to reflect the movement state of individual rings.

- **Topological structure proprieties and development**

The cuticle of the worm is stiff [14], however, the cells underneath the cuticle have relatively lower Yong's modulus [34] and are condensable during the movement of the worm. The puzzle type cell boundaries have multiple re – entrant angles (Figure 1*d*). The negative poisson's ratio structure [35] would increase the shear modulus [35] of the cell lattices. Thus, the Cambrian worm epithelium is more resistant to the shear force, and the shape of a cell within tissues can reflect the history of physical signals it encounters [36]. In the contract and elongation stage of the ring (Figure 4*f*), the big octagon cells have an opposite deformation direction to the small quadrangle cells [37], the anisotropy deformation forces may affect the distribution of cell proliferation events [38] within cell clusters.

The morphology of cells across boundary zones switches dramatically, indicating the fates of the cell-like structures are precisely determined. The energy – consuming mechanisms govern cell shape. The 4 – 8 cell lattices consist of puzzle type cells with negative Poisson's ratio, the structures display hystersis response to strong compression or elongation on the lattices [37]. Both the foam and puzzle type membranes are employed by modern cells [39]. The foam type cell predominate, ensuring flexibility during bending and facilitating a wide range of reshaping and rearrangement behaviors that are crucial to development and movement of the animals.

The developmental sequence of *Jinia* suggests the process by which the worms' rings elongate (Figure S1). On a larger scale, *Jinia* body elongation should start in the embryonic stages. If we treat *Markuelia* [40] as a model for the late embryonic stage of Cycloneuralia, we find each ring is approximately 20 micrometers in width which would occupy only two rows of cells [40]. Annelid segments can form from single-cell-wide precursors [9], and daughter cells emerge during the process of ring elongation (Figure S1*e-g*). The rosette pattern is treated as an intermediate phase of the elongation process [41]. The boundary cells constrain the cell flow within each ring, which may explain the rosette pattern formed near the boundary of the ring. Moreover, the boundary cells may promote the fluid-to-solid jamming transition underlies body axis elongation [42].

The study demonstrates the establishment of precise tissue boundary formation of early molting animals through the Cambrian – Early Ordovician period. The subdivision of the elongating body axis into repeated units is employed by dozens of phyla [43]. This framework restricts cell proliferation and force transmission within a segment, laying the foundation for functional differentiation among and within each unit of the animals body.

# Declarations

### Availability of data and materials

All fossil specimens from the Jindinshan and Meitan Formation are deposited in the collections of Guizhou Research Center for Palaeobiology, Guizhou University, Guizhou, China.


### Funding

This research is supported by the National Natural Science Foundation of China No.41902003 and Natural Science Foundation of Guizhou No. 20171057.

### Acknowledgment

I thank **Jonathan Payne** from Stanford University for his advice on the manuscript.


### Competing interests

The author declares no competing interests.

Contributions

TL designed the research. TL prepared the materials for the figures. TL wrote the manuscript with input from the DMM.

# References


1. Thompson, D. Arcy W. On growth and form. Cambridge: Univ. Press (1917)
2. Kesidis, G., Slater, B. J., Jensen, S., & Budd, G. E. (2019). Caught in the act: priapulid burrowers in early Cambrian substrates. *Proceedings of the Royal Society B*, *286*(1894), 20182505.
3. Liang, J., Balachandra, S., Ngo, S., & O'Brien, L. E. Feedback regulation of steady-state epithelial turnover and organ size. Nature, 548, 588. (2017)
4. Landsberg, K. P., Farhadifar, R., Ranft, J., et al. Increased cell bond tension governs cell sorting at the Drosophila anteroposterior compartment boundary. Current Biology 19, 1950–1955. (2009)
5. Roca-Cusachs, P., Conte, V., & Trepat, X. Quantifying forces in cell biology. Nature cell biology, 19(7), 742. (2017)
6. Sugimura, K., Lenne, P. F., & Graner, F. Measuring forces and stresses in situ in living tissues. Development, 143, 186-196. (2016)

7. Staple, D. B., Farhadifar, R., Röper, J. C., et al. (2010) Mechanics and remodelling of cell packings in epithelia. Eur. Phys. J. E 33, 117–127
8. Wang, D., Vannier, J., Yang, X., Sun, J., Sun, Y., Hao, W., Han, J. Cuticular reticulation replicates the pattern of epidermal cells in lowermost Cambrian scalidophoran worms. Proceedings of The Royal Society B: Biological Sciences, 287(1926), 20200470. (2020).
9. Oates, A. C., Morelli, L. G. & Ares, S. Patterning embryos with oscillations: structure, function and dynamics of the vertebrate segmentation clock. Development, 139, 625–639 (2012)
10. García-Bellido, D. C., Paterson, J. R. & Edgecombe, G. D. Cambrian palaeoscolecids (Cycloneuralia) from Gondwana and reappraisal of species assigned to Palaeoscolex. Gondwana Research 24, 780–795 (2013)
11. Hannibal, R. L., Price, A. L., & Patel, N. H. (2012). The functional relationship between ectodermal and mesodermal segmentation in the crustacean, Parhyale hawaiensis. *Developmental biology*, *361*(2), 427-438.
12. Hannibal, R. L., & Patel, N. H. (2013). What is a segment?. *EvoDevo*, *4*(1), 35.
13. Giangrande, A., & Gambi, M. C. (1998). Metamerism and life-style within polychaetes: Morpho-functional aspects and evolutionary implications. *Italian Journal of Zoology*, *65*(1), 39-50.
14. Muller, K. J. & Ingelore, H. Palaeoscolecid worms from the Middle Cambrian of Australia. Palaeontology 36, 549–591 (1993)
15. Wang, W., Muir, L. A., Botting, J. P., Feng, H., Servais, T., & Li, L. (2014). AT remadocian (E arly O rdovician) palaeoscolecidan worm from graptolitic shales in H unan P rovince, S outh C hina. *Palaeontology*, *57*(3), 657-671.
16. Wills, M. A., Gerber, S., Ruta, M., & Hughes, M. (2012). The disparity of priapulid, archaeopriapulid and palaeoscolecid worms in the light of new data. *Journal of evolutionary biology*, *25*(10), 2056-2076.
17. Fletcher, A. G., Osterfield, M., Baker, R. E., et al. Vertex models of epithelial morphogenesis. Biophysical journal 106, 2291–2304 (2014)
18. Grady, L. (2006). Random walks for image segmentation. *IEEE Transactions on Pattern Analysis & Machine Intelligence*, (11), 1768-1783.
19. Brodland, G. W., Veldhuis, J. H., Kim, S., et al. CellFIT: a cellular force-inference toolkit using curvilinear cell boundaries. PLoS One 9, e99116 (2014)
20. Bendix-Almgreen, Svend E., and John S. Peel. Hadimopanella from the Lower Cambrian of North Greenland: Structure and Affinities. 1988.
21. Topper, T. P., Brock, G. A., Skovsted, C. B., & Paterson, J. R. (2010). Palaeoscolecid scleritome fragments with Hadimopanella plates from the early Cambrian of South Australia. *Geological Magazine*, *147* (1), 86-97.
22. Liu Y, Wang Q, Shao T, et al. New material of three-dimensionally phosphatized and microscopic cycloneuralians from the Cambrian Paibian Stage of South China. Journal of Paleontology, 92: 87-98. (2018)

23. Botting, J. P., Muir, L. A., Van Roy, P., Bates, D., & Upton, C. (2012). Diverse middle Ordovician palaeoscolecidan worms from the Builth-Llandrindod Inlier of central Wales. *Palaeontology*, *55*(3), 501-528.
24. Conway Morris, S. The cuticular structure of the 495-Myr-old type species of the fossil worm Palaeoscolex, P. piscatorum (? Priapulida). Zoological Journal of the Linnean Society, 119, 69–82 (1997)
25. Hinz, I. , Kraft, P. , Mergl, M. , & KLAUS J. MüLLER. (2010). The problematic hadimopanella, kaimenella, milaculum and utahphospha identified as sclerites of palaeoscolecida. *Lethaia, 23* (2), 217-221.
26. Sugimura, K., Lenne, P. F., & Graner, F. Measuring forces and stresses in situ in living tissues. Development, 143, 186-196. (2016)
27. Kong, W. , Loison, O. , Shivakumar, P. C. , Chan, H. Y. , & Raphal Clément. (2019). Experimental validation of force inference in epithelia from cell to tissue scale. *entific Reports, 9*(1).
28. Gibson, M. C., Patel, A. B., Nagpal, R., et al. The emergence of geometric order in proliferating metazoan epithelia. Nature 442, 1038–1041 (2006)
29. Zhang, X. G., & Aldridge, R. J. Development and diversification of trunk plates of the Lower Cambrian lobopodians. Palaeontology, 50, 401-415. (2007)
30. Marinari, E., Mehonic, A., Curran, S., Gale, J., Duke, T., & Baum, B. (2012). Live-cell delamination counterbalances epithelial growth to limit tissue overcrowding. *Nature*, *484*, 542.
31. Caron, J. B., Smith, M. R., & Harvey, T. H. (2013). Beyond the Burgess Shale: Cambrian microfossils track the rise and fall of hallucigeniid lobopodians. *Proceedings of the Royal Society of London B: Biological Sciences*, *280* (1767), 20131613.
32. Heer, N. C. & Martin, A. C. Tension, contraction and tissue morphogenesis. Development 144, 4249–4260 (2017)
33. Lee, J. Y. & Goldstein, B. Mechanisms of cell positioning during C. elegans gastrulation. Development 130, 307–320 (2003)
34. Yang, C., Tibbitt, M. W., Basta, L., & Anseth, K. S. Mechanical memory and dosing influence stem cell fate. *Nature materials*, 13, 645. (2014)
35. Saxena, K. K., Das, R., & Calius, E. P. Three decades of auxetics research − materials with negative Poisson's ratio: a review. *Advanced Engineering Materials*, 18, 1847-1870. (2016)
36. Ron, A., Azeloglu, E. U., Calizo, R. C.,et al. Cell shape information is transduced through tension-independent mechanisms. *Nature communications*, 8, 2145. (2017)
37. Florijn, B., Coulais, C., & van Hecke, M. Programmable mechanical metamaterials. *Physical review letters*, 113, 175503 (2014)
38. LeGoff, L., Rouault, H., & Lecuit, T. A global pattern of mechanical stress polarizes cell divisions and cell shape in the growing Drosophila wing disc. *Development*, 140, 4051-4059. (2013)

39. Carter, R., Sánchez-Corrales, Y. E., Hartley, M., et al. Pavement cells and the topology puzzle. Development 144, 4386–4397 (2017)
40. Dong, X. P., Bengtson, S., Gostling, N. J., Cunningham, J. A., Harvey, T. H., Kouchinsky, A., ... & Donoghue, P. C. (2010). The anatomy, taphonomy, taxonomy and systematic affinity of Markuelia: Early Cambrian to Early Ordovician scalidophorans. *Palaeontology*, *53*(6), 1291-1314.
41. Tetley, R. J., & Mao, Y. (2018). The same but different: cell intercalation as a driver of tissue deformation and fluidity. *Phil. Trans. R. Soc. B*, *373*(1759), 20170328.
42. Mongera, A., Rowghanian, P., Gustafson, H. J., Shelton, E., Kealhofer, D. A., Carn, E. K., ... & Campàs, O. (2018). A fluid-to-solid jamming transition underlies vertebrate body axis elongation. *Nature*, *561*(7723), 401.
43. Davis, G. K. & Patel, N. H. The origin and evolution of segmentation.Trends in Genetics 15, 68–72 (1999)

# Figures

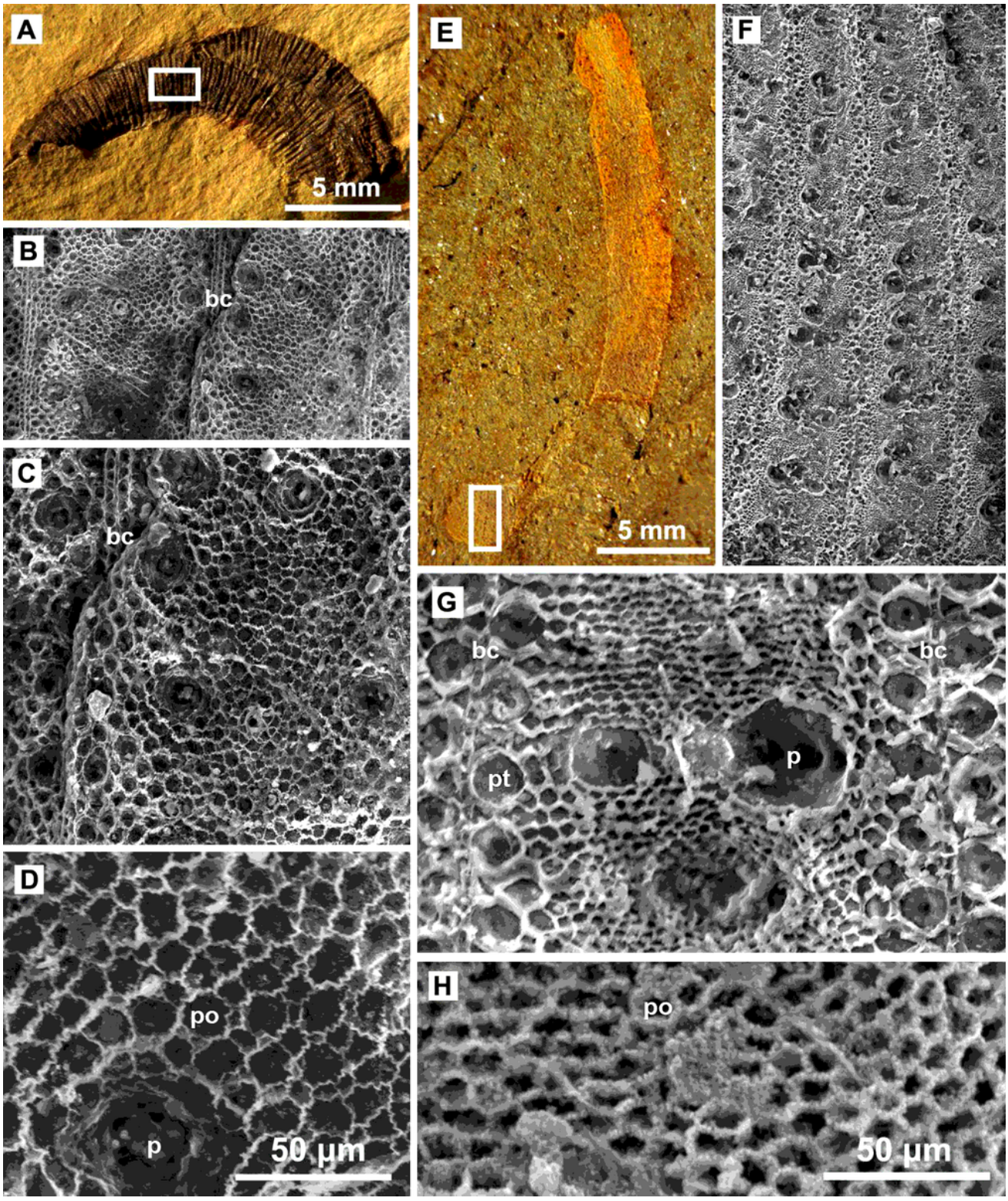


## Figure 1

Early worms epithelium. A–D GRCP 14001, Jinia rosettea gen. et sp. nov. from Cambrian Stage 4 (515 ma); B, zoom in of the square frame of A; C, zoom in of the epithelium overlapping region of B; D, zoom in of the 4-8 sides puzzle-type polygons; E–H GRCP 22001, Meitis elegans gen. et sp. nov. from Early Ordovician, Florian (470 ma). F, zoom in on the square frame of E. G, zoom in on a body unit of the worm,

showing 6 sides polygons and plates separated by tiny linear boundary cells; H, 6 sides polygons, some of which elongated along AP axis. Abbreviation: bc: boundary cell; p: plate; po: polygon; pt: platelet.

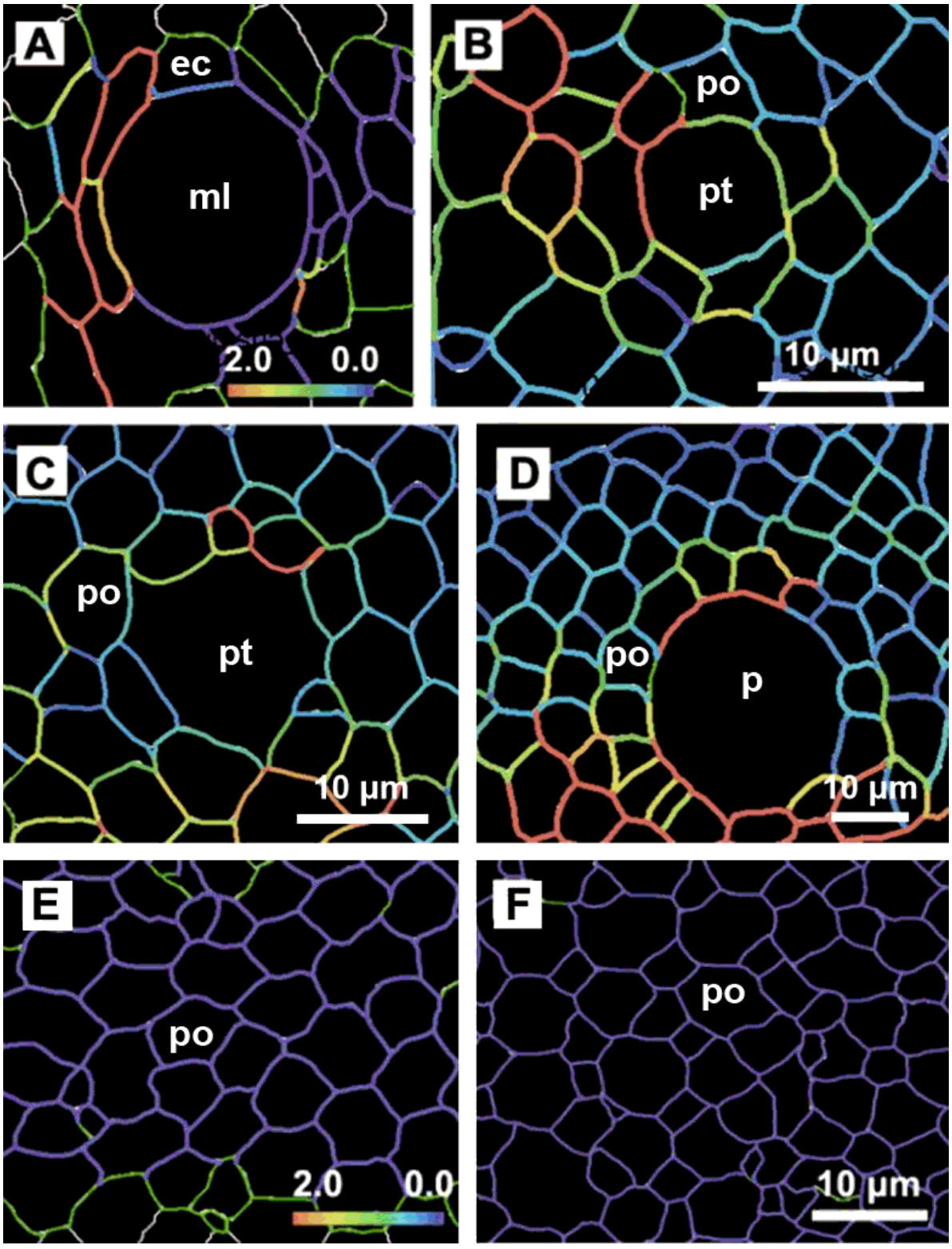


## Figure 2

The relative tension field of extant and extinct animals epithelium. A, The excited state of the tension field of mitosis loop of the extant animals epidermal cells28 and B–D the excited state of the tension field around the plate of Jinia rosettea. E, The ground state of the tension field of the generalize epidermal

cells of the Meitis elegans and F, J. rosettea. Abbreviation: ec: epithelial cell; ml: mitosis loop; p: plate; po: polygon; pt: platelet.

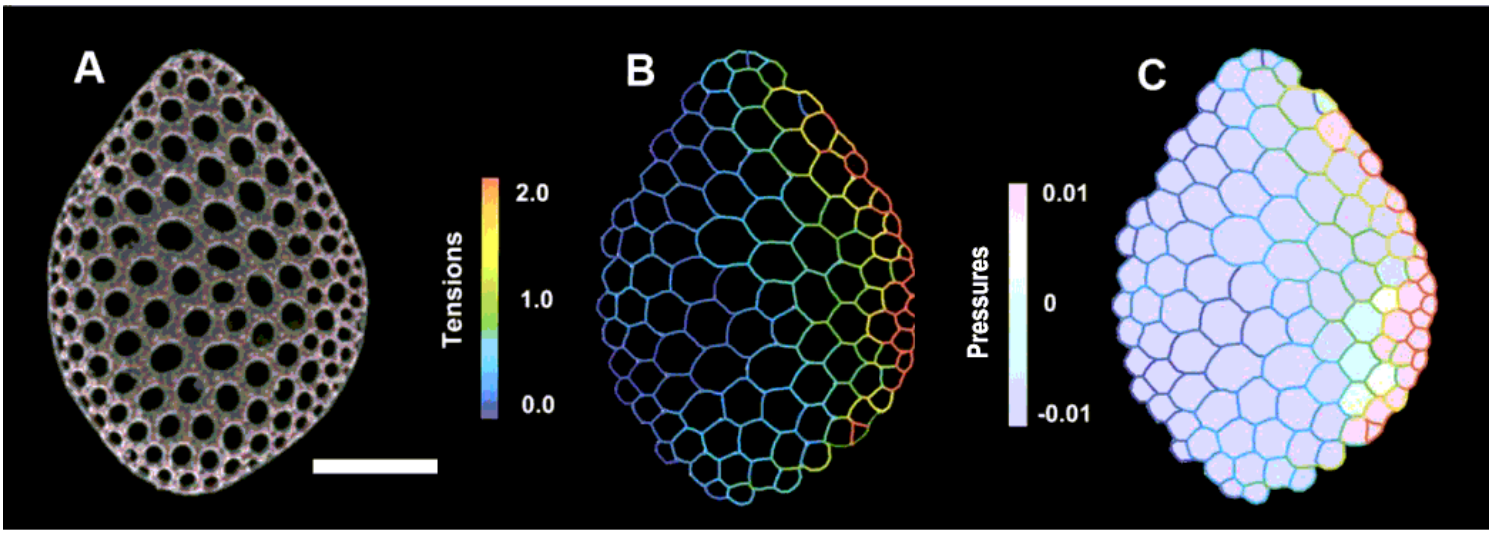


**Figure 3**

The relative tension field within the plates of the early Cambrian worms. A, RCCBYU 10491, Microdictyon jinshaense29 ; B, the tension field of RCCBYU 10491; C, the pressure field of RCCBYU 10491. Scale Bars: 200 μm.

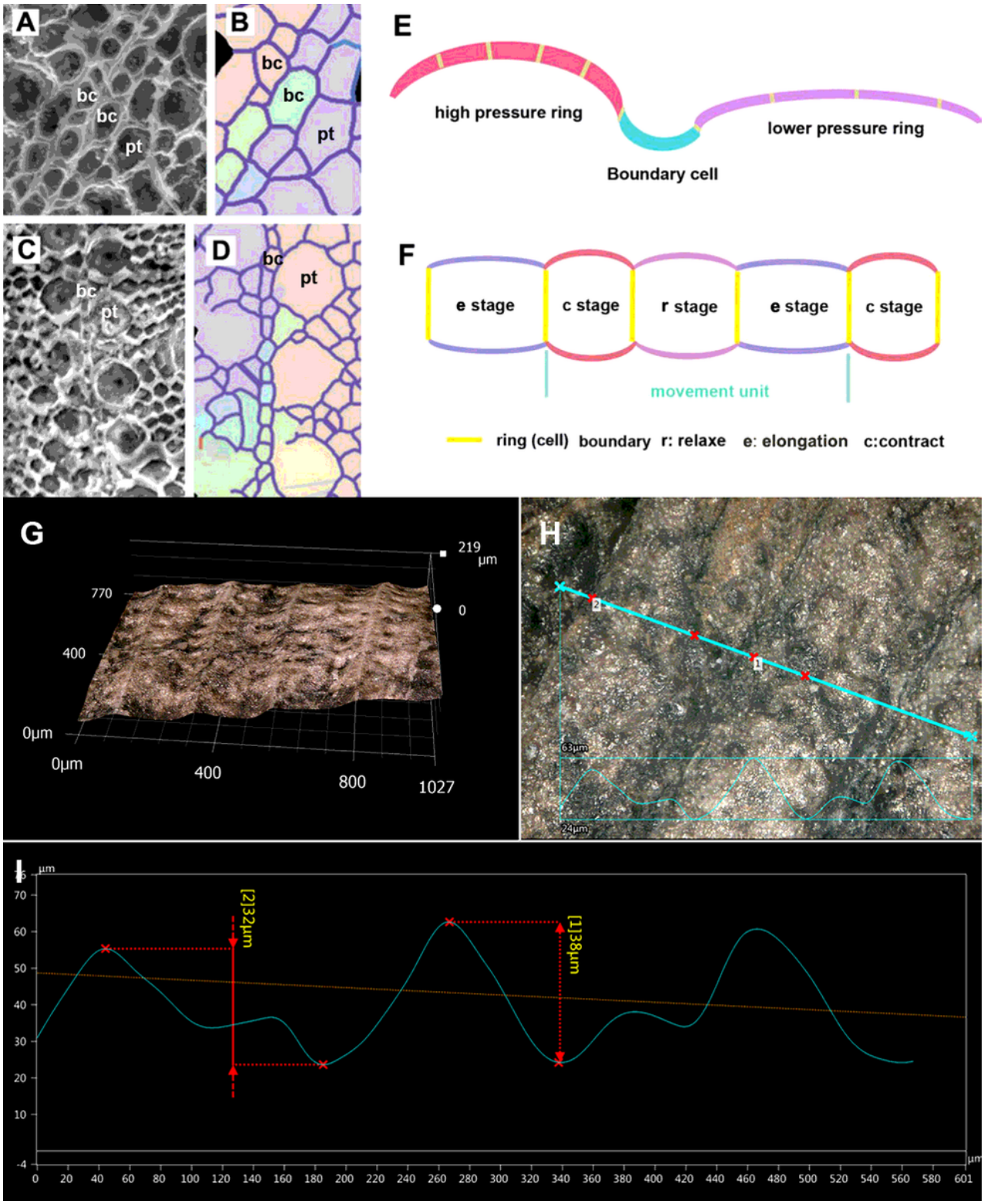


## Figure 4

The relative stress field of the boundary cells (BCs) region of the worms epithelium and their movement model. A–B, Jinia rosettea GRCP 14001; C–D, Meitis elegans GRCP 22001; E, sagittal plane sketch of the worm showing boundary cell maintain potential energy barrier between two rings; F, simplified peristalsis movement model of the worms. G, the hologram of J. rosettea GRCP 14001; H, I, the elevation landscape of the ring of J. rosettea. Abbreviation: bc: boundary cell; pt: platelet.

# Supplementary Files

This is a list of supplementary files associated with this preprint. Click to download.

- Supplementalinformation.docx